Optica Applicata, Vol. LIII, No. 3, 2023
DOI: 10.37190/oa230304

Aspherical, sphero-cylindrical, toroidal, and ellipsoidal surfaces for designing astigmatic spectacle lenses with axis orientation

Huazhong Xiang[1], Peng Wang[1], Zexi Zheng[2,*], Gang Zheng[1,3], Jiabi Chen[3], Cheng Wang[1], Dawei Zhang[3,4], Songlin Zhuang[3,4]

[1]School of Health Science and Engineering, University of Shanghai for Science and Technology, Shanghai 200093, China

[2]School of Mechanical Engineering, University of Shanghai for Science and Technology, Shanghai 200093, China

[3]School of Optical-Electrical and Computer Engineering, University of Shanghai for Science and Technology, Shanghai 200093, China

[4]Engineering Research Center of Optic Instrument and System, Shanghai Engineering University of Shanghai for Science and Technology, Shanghai 200093, China

[*]Corresponding author: zexizheng@outlook.com

In this paper, formulas for aspherical, sphero-cylindrical, toroidal, and ellipsoidal surfaces with astigmatic axes are derived. Based on this, four types of curved surfaces were designed to correct astigmatism with axis, and, subsequently, the lenses were simulated, fabricated, and measured. A total of ten spectacle lenses in two groups were designed. Those in the first group used identical optical parameters. The spherical and cylindrical powers and maximum and minimum edge thicknesses of aspherical, sphero-cylindrical, and ellipsoidal surfaces were compared. The results indicated that the power of the lens constructed using the toroidal surface was more accurate than those of the other three lenses. Moreover, the minimum edge thickness of the toroidal surface was 1.2%, 4.98%, and 4.87% lower than those of the aspherical, sphero-cylindrical, and ellipsoidal surfaces, respectively. The powers and edge thicknesses of toroidal surfaces with different diopters were compared in the second group. The minimum and maximum edge thicknesses were observed to be reduced by 8.97% and 6.05%, respectively, corresponding to the conic constants obtained via ray tracing. The conclusion will be significant for clinical ophthalmology and optical design for the patients with astigmatism.

Keywords: toric, astigmatism, spherocylinder, aspheric, ellipsoidal surface.

1. Introduction

Astigmatism is a refractive error in which parallel rays of light entering the eye focus on two distinct focal lines perpendicular to each other, rather than to a single focal point [1].

Regular astigmatism can be classified into three categories: with-the-rule (WTR) (+ cylinder axis 90 ± 15 degrees), against-the-rule (ATR) (+ cylinder axis 180 ± 15 degrees), and oblique (OBL) (all other orientations) [2]. The optical blur induced by uncorrected astigmatism may trigger the development of myopia [3]. Approximately 14.9% of children suffer from astigmatism globally [4, 5].

Currently, spectacle lenses, contact lenses, and surgical correction (*e.g.*, cataract surgery and corneal refractive surgery) are the only available modes of clinical treatment for astigmatism correction [1]. Cylindrical lens has dioptric power only on one principal meridian, so for astigmatic eyes, it is necessary to correct two different principal meridians of the eye through spherical cylindrical lens [6]. However, accurate definition of sphero-cylindrical surfaces to obtain optimal correction in specific cases is often difficult and complex [7]. In a toric lens, the cylindrical component accounts for the difference between the base curve and the cross curve, *i.e.*, the power to be added to the base curve to produce the cross curve. This is different from the case of a sphero -cylindrical lens [8]. MURRAY generalized a ray incident on any point of the toric surface from any direction based on a skew ray traced through a toric surface [9]. FOWLER evaluated sphero-cylindrical components of a toroidal surface by measuring curvature along three meridians intersecting at angles of 60° with respect to each other [10]. LANDGRAVE *et al*. proposed equations for the sagitta, the unit normal vector, and the principal curvatures of a toroidal surface appropriate for all tracing purposes. He also derived equations corresponding to a revolving curve shaped like a conic section, based on which the equations corresponding to a toric surface can be readily deduced [11]. Further, it has been observed that (i) an ellipsoid is a better than spherical, toric, or parabolic lenses in approximation of the corneal surface in the human eye, and (ii) contact lenses with inner elliptical surfaces exhibit marked improvements in terms of comfort of the wearer and durability [12]. REMÓN *et al*. found that when accommodation is not active, the influence of the cylinder axis is of less importance than other clinical variables such as the selected visual acuity (VA) chart. Moreover, the same astigmatic error (same power and axis) induced in different eyes provides VA variations of higher amount than those provided by astigmatism of the same power and different axes induced in the same eye [13]. KOBASHI *et al*. reported that oblique astigmatism had lower VA and reading performance than those with uncorrected 0° and 90° axis of astigmatism [14]. ATCHISON *et al*. found that subjective blur-limits for cylinder at 0° axis, were greater (about 20%) than those for oblique axes [15]. MATHUR *et al*. found that VA was affected significantly by the axis of the cylinder, with better VA for 90° than for any other orientation (45°,135°, and 180°) [16]. MIMOUNI *et al*. evaluated the effect of astigmatism axis on uncorrected distance visual acuity (UDVA) in emmetropic eyes that underwent laser refractive surgery and found the astigmatic axis has a small but significant effect on UDVA in emmetropic eyes [17]. PUJOL *et al*. reported that when a spherocylindrical lens to correct the astigmatism is placed in front of the eye, with an angle formed by the lens and the eye axis other than zero, the lens–eye system has a residual spherocylindrical refractive error [18]. MILLER *et al*. found that the subjects reported discomfort with astigmatic errors of 0.50 D (diopter) but the level of discom-

fort was dependent on the axis of astigmatism [19]. Therefore, the orientation of the astigmatic axis may play an essential role in visual performance in astigmatic eyes and it is important to correct astigmatic axis for spectacle lenses.

In this study, we derive and compare the formulas of aspherical, sphero-cylindrical, toroidal, and ellipsoidal surfaces with astigmatic axes to design astigmatic spectacle lenses. Based on this, four types of curved surfaces are designed, simulated, fabricated, and measured. In aggregate, two groups of ten astigmatic lenses are designed. The first group includes aspherical, toroidal, sphero-cylindrical, and ellipsoidal surfaces, which share identical parameters. Following the design and manufacture of this group, the toroidal surfaces corresponding to different spherical powers are combined with the astigmatism of –2 D (diopter) along an axis orientated at an angle of 75°. After the design of all constituents of the two groups, the optical properties and maximum and minimum edge thicknesses of all lenses are compared. The astigmatic spectacle lenses are measured by using the VM-2500. The results between the production and theoretical reveals that lenses of both groups are comparable in terms of spherical and cylindrical powers.

The remainder of this paper is organized as follows. The different principles of astigmatic optical surfaces are described briefly in Section 2. The experimental results are presented and discussed in Section 3. Finally, the conclusions of this study are presented in Section 4.

2. Principles of different astigmatic optical surfaces

Spectacle lenses are designed using a three-dimensional right-handed orthogonal coordinate system, where the *Z*-axis is the optical axis. The origin of the coordinates system is chosen to be coincident with the vertex of the aspheric surface. Let us denote spherical power by S and cylindrical power by C.

$$\begin{cases} c_x = S/(n-1) \\ c_y = (S+C)/(n-1) \end{cases} \tag{1}$$

where n denotes the refractive index of the material, c_x denotes the curvature on the XZ plane, and c_y denotes the curvature on the YZ plane.

The origin is denoted by O, and the Z axis is assumed to be aligned along the direction from O to the center of the lens. The XYZ Cartesian system is supplemented using a cylindrical $X'Y'Z'$ coordinate system, in which θ denotes the orientation of the cylindrical system with respect to the *x*-*z* plane, as depicted in Fig. 1.

Thus, θ denotes the axial position recorded in the prescription (relaxing the requirement such that $0 < \theta \leq 180°$).

$$\begin{cases} x' = x\cos\theta - y\sin\theta \\ y' = x\sin\theta + y\cos\theta \end{cases} \tag{2}$$

where x' and y' are obtained by rotating x and y by θ.

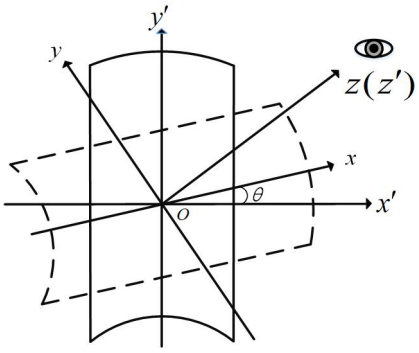

Fig. 1. Orientation of the cylindrical lens.

The sphero-cylindrical surface can be described using the following equation [9]:

$$z_{\mathrm{s}} = \frac{c_x x'^2 + c_y y'^2}{1 + \left\{1 - \left[(1+k_x)c_x x'^2 + (1+k_y)c_y y'^2\right]^2 / (x'^2 + y'^2)\right\}^{1/2}} \tag{3}$$

where z denotes the sagittal height, c_x denotes the curvature on the $X'Z'$ plane (semi -diameter of the torus), c_y denotes the curvature on the $Y'Z'$ plane, x and y denote the x- and y-coordinates, and k_x and k_y denote the conic constants along the X' and Y' axes, respectively.

Thus, using Eqs. (2) and (3), we can deduce that the sphero-cylindrical surface, which is given by the following equation in the XYZ coordinate system:

$$Z_{\mathrm{s}} = \frac{c_x (x\cos\theta - y\sin\theta)^2 + c_y (x\sin\theta + y\cos\theta)^2}{1 + \left\{1 - \dfrac{\left[(1+k_x)c_x (x\cos\theta - y\sin\theta)^2 + (1+k_y)c_y (x\sin\theta + y\cos\theta)^2\right]^2}{(x\cos\theta - y\sin\theta)^2 + (x\sin\theta + y\cos\theta)^2}\right\}^{1/2}} \tag{4}$$

Similarly, the equation of the regular toroidal surface in the $X'Y'Z'$ coordinate system is given by the biconic type [9]:

$$z_{\mathrm{t}} = \frac{c_x x'^2 + c_y y'^2}{1 + \left[1 - (1+k_x)c_x^2 x'^2 - (1+k_y)c_y^2 y'^2\right]^{1/2}} \tag{5}$$

Thus, the following expression for the toroidal surface in the XYZ coordinate system can be deduced by combining Eqs. (2) and (5):

$$Z_{\mathrm{t}} = \frac{c_x(x\cos\theta - y\sin\theta)^2 + c_y(x\sin\theta + y\cos\theta)^2}{1 + \left[1 - (1+k_x)c_x^2(x\cos\theta - y\sin\theta)^2 - (1+k_y)c_y^2(x\sin\theta + y\cos\theta)^2\right]^{1/2}} \tag{6}$$

Finally, the expression for the regular ellipsoidal surface in the $X'Y'Z'$ coordinate system is given by [9]

$$z_{\mathrm{e}} = \frac{c_x x'^2 + c_y y'^2}{1 + \left\{1 - c_x\left[(1+k_x)c_x x'^2 + c_y y'^2\right]\right\}^{1/2}} \tag{7}$$

Thus, its expression in the XYZ system can be derived based on Eqs. (2) and (7):

$$Z_{\mathrm{e}} = \frac{c_x(x\cos\theta - y\sin\theta)^2 + c_y(x\sin\theta + y\cos\theta)^2}{1 + \left\{1 - c_x\left[(1+k_x)c_x(x\cos\theta - y\sin\theta)^2 + c_y(x\sin\theta + y\cos\theta)^2\right]\right\}^{1/2}} \tag{8}$$

where k_x and k_y are obtained via ray tracing.

These surfaces are generated by the rotation of a function about an axis of symmetry passing through the optical axis and perpendicular to it.

3. Results and discussion

3.1. Optical parameters and simulations

The values of the optical parameters of spectacle lenses are listed in Table 1. Aspherical, sphero-cylinder, toroidal, and ellipsoidal surfaces in the first group were utilized

T a b l e 1. Optical parameters of spectacle lenses used to correct astigmatism (unit: D, 1/m).

Group	SPH [D]	CYL [D]	Axis [deg]	*n*	Rf [mm]	CT [mm]	CRIB [mm]
Group 1	–8.00	–2.00	75	1.67	303.30	1.20	70
	–8.00	–2.00	75	1.67	303.30	1.20	70
Group 2	–7.00	–2.00	75	1.67	303.30	1.20	70
	–6.00	–2.00	75	1.67	303.30	1.20	70

SPH: sphere diopter; CYL: cylinder diopter; *n*: refractive index; Axis: axis of astigmatism; Rf: front surface radius associated to an lens with a refractive index, $n = 1.552$; CT: central thickness; CRIB: crib diameter.

to design astigmatic spectacle lenses using identical parameters, while those in the second group were used to design astigmatic spectacle lenses of various diopters using toroidal surfaces.

3.1.1. Simulations corresponding to the first group

Simulations of the aspherical, toroidal, sphero-cylindrical, and ellipsoidal surfaces are depicted in Fig. 2. The simulations were conducted using the freeform verifier (FFV) software (ROTLEX, Israel), which is a commercial software used as a moiré deflectometer with a point source. Moiré fringes are produced when a pitch grating is superimposed on another pitch grating at a smaller angle. The angle between the interfering gratings was maintained to be constant in the ROTLEX systems. A circle with a diameter of 60 mm, which is much larger than the spectacle frame, was taken to be the observation window. The photometric gradient was 0.25 diopter.

The maps of the power distribution are in agreement with the expectations in the viewing zones in every simulation. Table 2 shows that the differences in spherical pow-

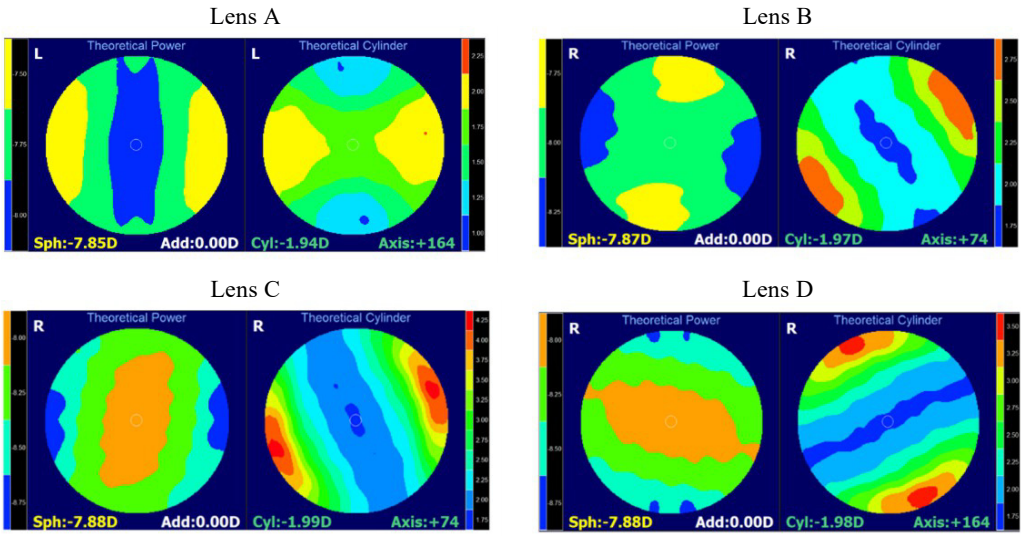

Fig. 2. Simulation of sphere (left) and cylinder (right) to an aspherical surface, a sphero-cylindrical surface, a toroidal surface and an ellipsoidal surface for lens A, B, C and D, respectively. Sph: spherical power; Add: additional power; Cyl: cylindrical power; Axis: the axis of astigmatism.

T a b l e 2. Simulation results for astigmatic spectacle lenses in the first group (unit: D, 1/m).

Lens	Surface	SPH [D]	CYL [D]	Axis [deg]
A	Aspherical	–7.85	–1.94	164
B	Sphero–cylindrical	–7.87	–1.97	74
C	Toroidal	–7.88	–1.98	164
D	Ellipsoidal	–7.88	–1.99	74

SPH: sphere; CYL: cylinder.

er of the aspherical, sphero-cylindrical, toroidal, and ellipsoidal surfaces were –0.15, –0.13, –0.12, and –0.12 D, respectively, while those in cylindrical power were –0.06, –0.03, –0.02, and –0.01 D, respectively. The difference in the axis orientation used by the four design methods was 1°. These values are in close agreement with the theoretical spherical and cylindrical powers and the theoretical axis orientations. Thus, the proposed designs were found to be suitable for a wearer with astigmatism. As the difference between the spherical and cylindrical powers was the smallest in the case of the toroidal surface, this result was used to design lenses in the second group.

3.1.2. Simulations corresponding to the second group

The simulations using toroidal surfaces of varying diopters are depicted in Figs. 3–7.

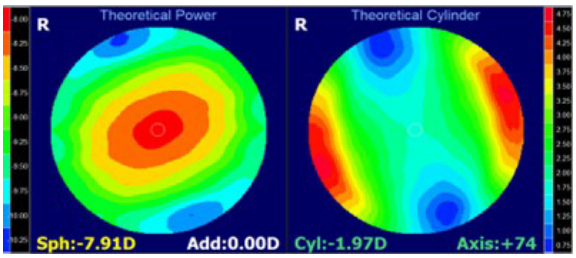

Fig. 3. Simulation of sphere (left) and cylinder (right) corresponding to a –8.00DS/–2.00DC×75° toroidal surface (k_x, $k_y = 0$) for lens E.

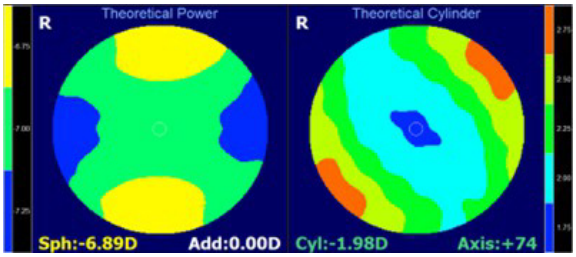

Fig. 4. Simulation of sphere (left) and cylinder (right) corresponding to a –7.00DS/–2.00DC×75° toroidal surface (k_x, $k_y \neq 0$) for lens F.

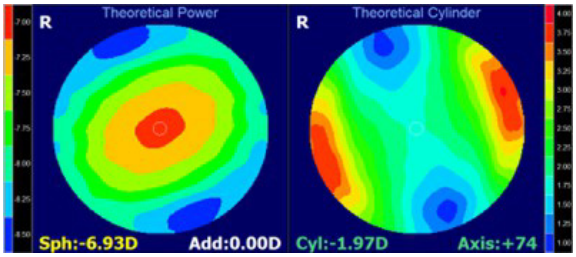

Fig. 5. Simulation of sphere (left) and cylinder (right) corresponding to a –7.00DS/–2.00DC×75° toroidal surface (k_x, $k_y = 0$) for lens G.

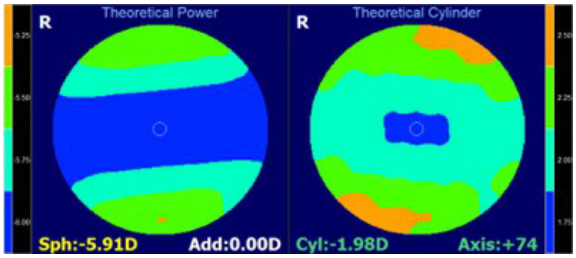

Fig. 6. Simulation of sphere (left) and cylinder (right) corresponding to a –6.00DS/–2.00DC×75° toroidal surface (k_x, $k_y \neq 0$) for lens H.

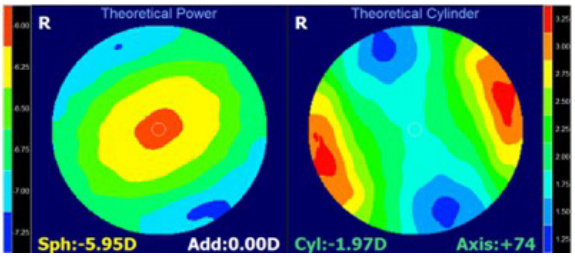

Fig. 7. Simulation of sphere (left) and cylinder (right) corresponding to a –6.00DS/–2.00DC×75° toroidal surface (k_x, $k_y = 0$)for lens I.

T a b l e 3. Simulation results corresponding to astigmatic spectacle lenses in the second group (unit: D, 1/m).

Lens	k_x, k_y	SPH [D]	CYL [D]	Axis [deg]
C	≠	–7.88	–1.98	164
E	0	–7.91	–1.97	74
F	≠	–6.89	–1.98	74
G	0	–6.93	–1.97	74
H	≠	–5.91	–1.98	74
I	0	–5.95	–1.97	74

SPH: sphere diopter; CYL: cylinder diopter; Axis: axis of astigmatism.

The lens C was used as a reference lens. Its characteristics, in combination with the results depicted in Figs. 3–7, are listed in Table 3.

Figures 3–7 verify that the power distributions are in agreement with the expectations in the viewing zones in every simulation. The differences in spherical power of the toroidal surfaces considered in Figs. 3–7 were –0.09, –0.11, –0.07, –0.09, and –0.05 D, respectively, while those in cylindrical powers were –0.03, –0.02, –0.03, –0.02, and –0.03 D, respectively. The difference between the orientations of the axes of the toroidal surfaces was 1°. The accuracy of the spherical and cylindrical power was observed to depend on k_x and k_y.

3.2. Analysis of optical properties

The manufacturing process for the posterior surface utilized a computer numerical control (CNC) optical generating machine of Satisloh VFT-orbit (Jiangsu Mingyue Photoelectric Technology Co. Ltd., China) for turning, milling, grinding, and polishing. Figure 8 depicts the four different spectacle lenses in the first group. Figure 9 depicts the six different lenses in the second group.

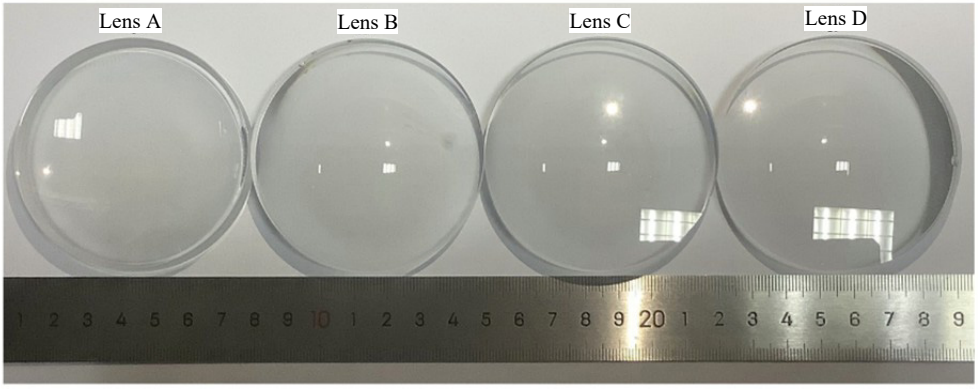

Fig. 8. Four different spectacle lenses in first group.

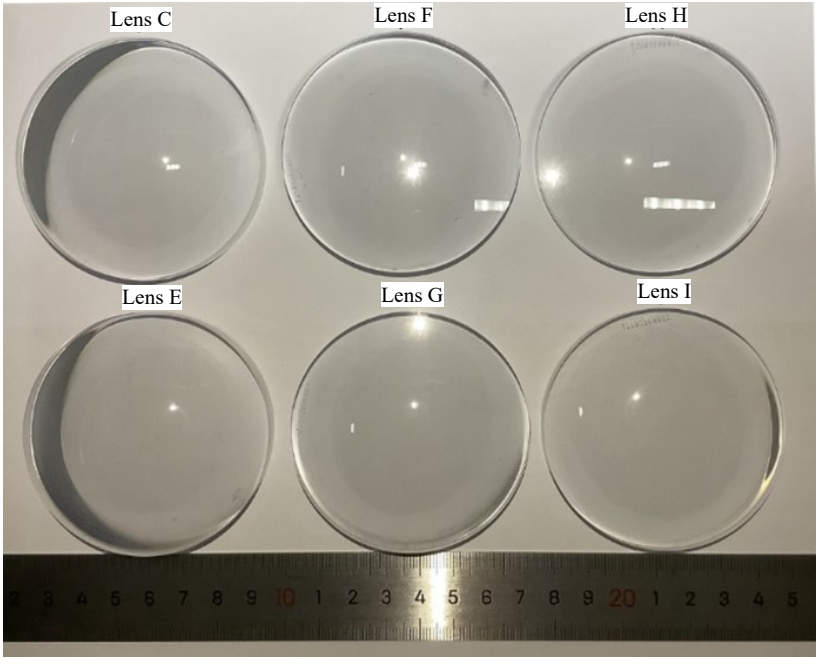

Fig. 9. Six different spectacle lenses in second group (the lens C was used as a reference lens).

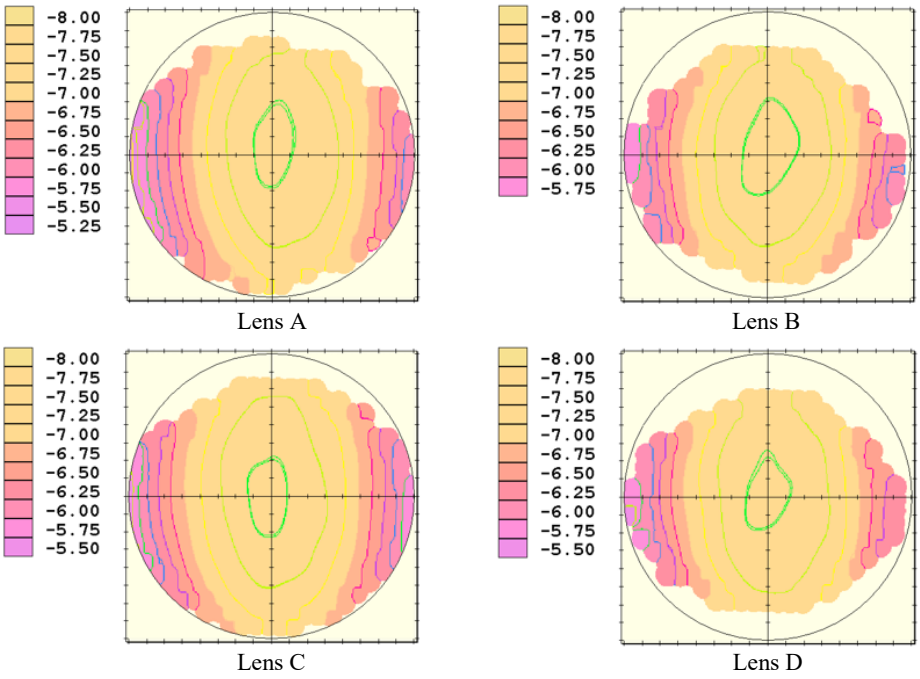

Fig. 10. Contour plots of spherical power of lenses in the first group.

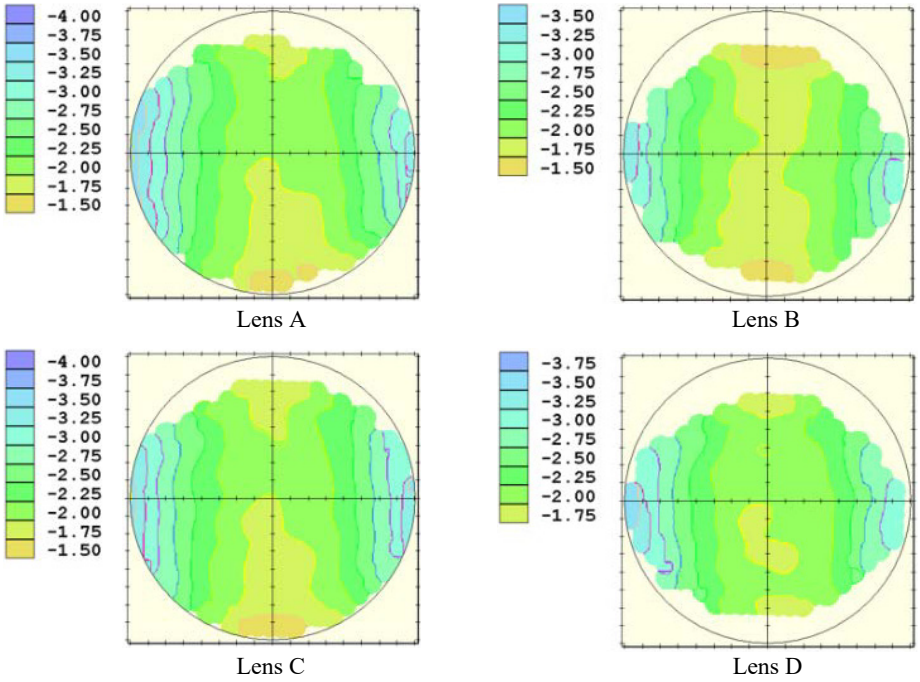

Fig. 11. Contour plots of cylindrical power of lenses in the first group.

T a b l e 4. Measurements of spectacle lenses in first group.

Lens	Surface	SPH [D]	CYL [D]	CT [mm]	ETmin [mm]	ETmax [mm]
A	Aspherical	–8.08	–1.97	1.20	8.31	10.48
B	Sphero-cylindrical	–8.09	–1.98	1.20	8.64	11.01
C	Toroidal	–8.00	–1.99	1.20	8.21	10.60
D	Ellipsoidal	–8.01	–2.02	1.20	8.63	11.16

SPH: sphere diopter, CYL: cylinder diopter, CT: central thickness, ETmin: minimum edge thickness, ETmax: maximum edge thickness.

The lenses were inspected using a Visionix VM2500 lens power mapper (France) and NIDEK's LM-1800P lensmeter (Japan). Figures 10 and 11 present the contour plots of the average spherical and cylindrical powers (astigmatism), respectively, of spectacle lenses in the first group. Figures 12 and 13 present the contour plots of the average spherical and cylindrical powers (astigmatism), respectively, of spectacle lenses in the second group. The contour lines are at intervals of 0.25 D for the spectacle lenses in the first and second groups. The lens diameter was set to be 50 mm. The lenses were not in the axial position during measurement.

Figures 10 and 11 depict the different power distribution maps (average spherical and cylindrical powers) of the aspherical, sphero-cylindrical, toroidal, and ellipsoidal surfaces, where the luminosity varies smoothly from the center to the edge. The measurements listed in Table 4 reveal that the spherical and cylindrical power distributions of the four lenses are relatively similar. The differences in spherical power corresponding to the four lenses were –0.08, –0.09, –0.00, and –0.01 D, while those in cylindrical power were –0.03, –0.02, –0.01, and –0.02 D. Thus, the spherical and cylindrical powers of the toroidal surface were more accurate than those of other surfaces. The minimum edge thickness of the toroidal surface was 1.20%, 4.98%, and 4.87% thinner than that of the aspherical surface, sphero-cylindrical surface, and the ellipsoidal surface, respectively. The maximum edge thickness of the aspherical surface was 4.81%, 1.13%, and 6.09% thinner than that of the sphero-cylindrical surface, surface, and the ellipsoidal surface, respectively. Therefore, the minimum edge thickness of the toroidal surface was less than that of the other surfaces, and the maximum edge thickness of the aspherical surface was less than that of the other surfaces. However, the maximum edge thickness of the toroidal surface was the second-lowest.

Figures 12 and 13 depict the spherical and cylindrical power distribution maps corresponding to toroidal surfaces with different diopters, and the diopter variations are smooth from the center to the edge of the image. The measurements listed in Table 5 reveal that the differences in spherical power between the lenses from C and E–F in order were 0.00, –0.03, 0.00, –0.02, –0.02, and –0.04 D, respectively, and the differences in cylindrical power lenses were –0.01, –0.14, –0.01, –0.02, –0.01, and –0.05 D, respectively. The minimum and maximum edge thicknesses of the lens C, were 9.38% and 5.86% thinner than those of the lens F, respectively, which were, in turn, 7.10% and 5.39% thinner than those of the lens G, respectively. The minimum and maximum

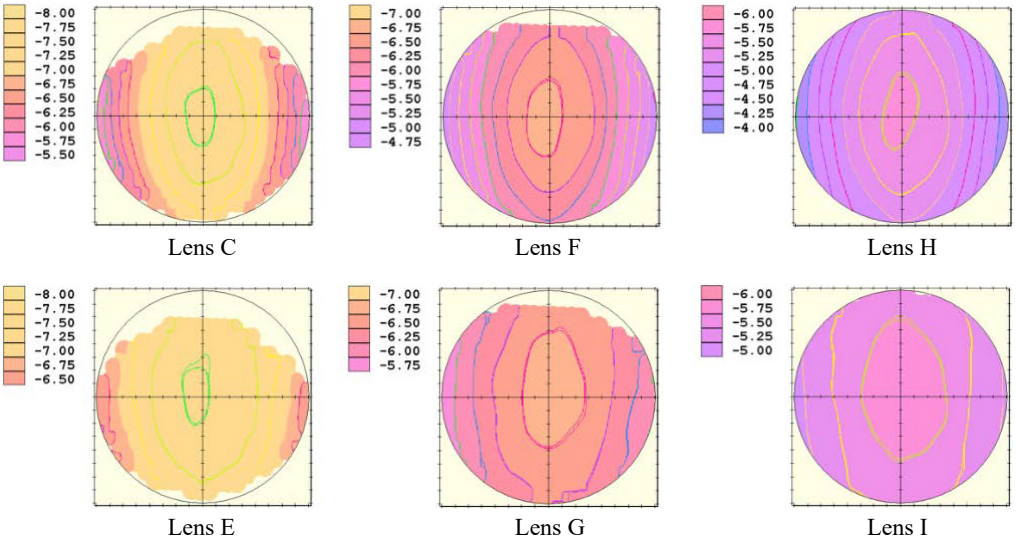

Fig. 12. Contour plots of spherical power of lenses in the second group.

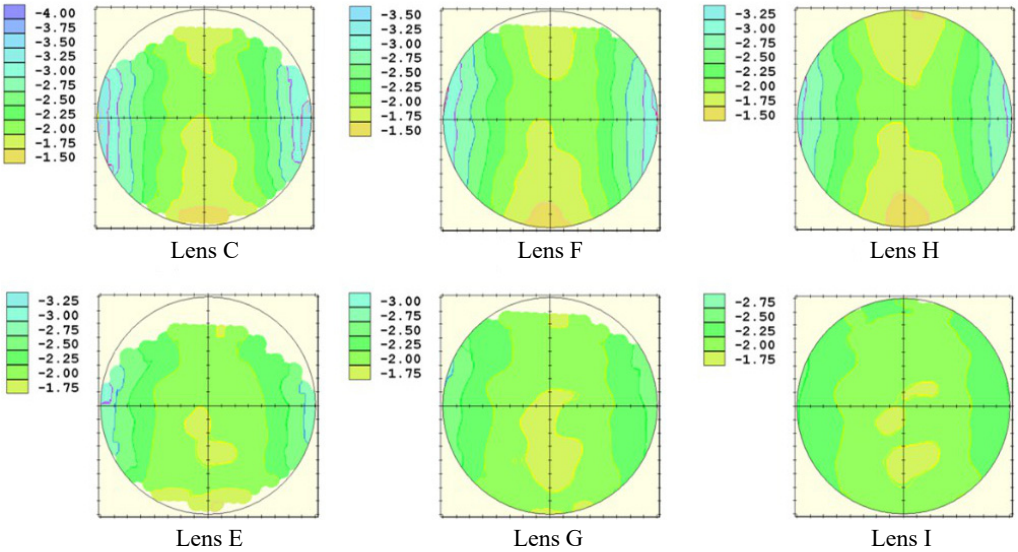

Fig. 13. Contour plots of cylindrical power of lenses in the second group.

edge thicknesses of the lens H, were 10.44% and 6.90% thinner than those of the lens I, respectively. Therefore, the minimum and maximum edge thicknesses of the toroidal surface can be reduced by calculating k_x and k_y using the ray-tracing method.

The observations of this study were compared to those obtained by techniques proposed by XIANG *et al*. [12], in which toroidal, sphero-cylindrical, ellipsoidal, and com-

T a b l e 5. Measurements of spectacle lenses in second group.

Lens	k_x, k_y	SPH [D]	CYL [D]	CT [mm]	ETmin [mm]	ETmax [mm]
C	$\neq 0$	–8.00	–1.99	1.20	8.21	10.60
E	$= 0$	–7.97	–2.14	1.20	9.06	11.26
F	$\neq 0$	–7.00	–1.99	1.20	7.33	9.48
G	$= 0$	–6.98	–1.98	1.20	7.89	10.02
H	$\neq 0$	–5.98	–1.99	1.20	6.09	8.23
I	$= 0$	–5.96	–2.05	1.20	6.80	8.84

SPH: sphere diopter, CYL: cylinder diopter, CT: central thickness, ETmin: minimum edge thickness, ETmax: maximum edge thickness.

bined surfaces were used to correct astigmatism in aspheric spectacle lenses. Further, the differences between the proposed techniques were analyzed. The toroidal lens helped to extend the range of clear vision surrounding the lens. In contrast, the ellipsoidal and sphero-cylindrical surfaces achieved more accurate centering of the lens around the optical axis of the eye, avoided astigmatism, and provided better visual perception. Compared to the study published by MALACARA *et al*. [20], four different astigmatic lenses were manufactured in this study and their optical properties were compared. The use of each of these surfaces was internally defined, and the analytical expressions of the four different astigmatic surfaces were clearly presented. The results indicate that the proposed method enables the flexible selection of any of the lenses considered in this study by optical design developers.

4. Conclusions

In this study, formulas for aspherical, sphero-cylindrical, toroidal, and ellipsoidal surfaces with astigmatic axes were derived and compared. Based on this, four types of curved surfaces were designed to correct astigmatism and axis, their performances were simulated, and the lenses were fabricated and measured. In aggregate, ten lenses were manufactured in two groups using a CNC optical generating machine and they were measured using VM-2500. Equivalent power contour plots for spherical and cylindrical powers were estimated and compared using the VM-2500. We observed that all 10 spectacle lenses and the minimum and maximum edge thicknesses exhibited some common characteristics.

In particular, the following conclusions were derived:

1. The test results indicated that the toroidal surface is better suited to correct astigmatism compared to aspherical, sphero-cylindrical, and ellipsoidal surfaces as its axis orientation, photometric accuracy, and minimum edge thickness are better than those of the other three surfaces.

2. The minimum and maximum edge thicknesses were observed to be reduced by 8.97% and 6.05%, respectively, corresponding to the conic constants obtained via ray tracing on average.

3. Different design methods exhibited different conic constants along different directions, which can be leveraged to reduce the edge thickness or increase the size of the central focal area. Thus, these can be tailored to satisfy specific demands.

In this paper, we assumed that conic constants were obtained via ray tracing. In future studies, we intend to consider different conic constants and incorporate more complicated design objectives, *e.g.*, superimpositions on other free-form surfaces, such as progressive lenses, within the method.

Disclosures

The authors declare no conflicts of interest.

Acknowledgements

Manufacturing and measuring equipment was provided by Jiangsu Mingyue Photoelectric Technology Co. Ltd, and by the National Natural Science Foundation of China (No. 61605114 and No. 52206102).

References

[1] READ S.A., VINCENT S.J., COLLINS M.J., *The visual and functional impacts of astigmatism and its clinical management*, Ophthalmic and Physiological Optics **34**(3), 2014: 267-294. https://doi.org/10.1111/opo.12128

[2] YAMAMOTO T., HIRAOKA T., BEHEREGARAY S., OSHIKA T., *Influence of simple myopic against-the-rule and with-the-rule astigmatism on visual acuity in eyes with monofocal intraocular lenses*, Japanese Journal of Ophthalmology **58**(5), 2014: 409-414. https://doi.org/10.1007/s10384-014-0337-1

[3] READ S.A., COLLINS M.J., CARNEY L.G., *A review of astigmatism and its possible genesis*, Clinical and Experimental Optometry **90**(1), 2007: 5-19. https://doi.org/10.1111/j.1444-0938.2007.00112.x

[4] HASHEMI H., FOTOUHI A., YEKTA A., PAKZAD R., OSTADIMOGHADDAM H., KHABAZKHOOB M., *Global and regional estimates of prevalence of refractive errors: Systematic review and meta-analysis*, Journal of Current Ophthalmology **30**(1), 2018: 3-22. https://doi.org/10.1016/j.joco.2017.08.009

[5] FOZAILOFF A., TARCZY-HORNOCH K., COTTER S., WEN G., LIN J., BORCHERT M., AZEN S., VARMA R., *Prevalence of astigmatism in 6- to 72-month-old African American and Hispanic children: The multi-ethnic pediatric eye disease study*, Ophthalmology **118**(2), 2011: 284-293. https://doi.org/10.1016/j.ophtha.2010.06.038

[6] JALIE M., *Modern spectacle lens design*, Clinical and Experimental Optometry **103**(1), 2020: 3-10. https://doi.org/10.1111/cxo.12930

[7] BAUDE D., CHAVEL P., JOYEUX D., TABOURY J., *Optical lens for correcting astigmatism*, U.S. Patent, 5,016,977 (1991).

[8] JALIE M., *The Principles of Ophthalmic Lenses*, 4th Ed., Association of Dispensing Opticians, London, 1984.

[9] MURRAY A.E., *A toric skew ray trace*, Journal of the Optical Society of America **44**(9), 1954: 672-676. https://doi.org/10.1364/JOSA.44.000672

[10] FOWLER C.W., *Assessment of toroidal surfaces by the measurement of curvature in three fixed meridians*, Ophthalmic and Physiological Optics **9**(1), 1989: 79-80. https://doi.org/10.1111/j.1475-1313.1989.tb00812.x

[11] LANDGRAVE J.E.A., VILLALOBOS A., GONZÁLEZ C., *Simple mathematical representation of toroidal surfaces*, Proceedings of the SPIE, Vol. 6046, Fifth Symposium Optics in Industry, 2006: 604601. https://doi.org/10.1117/12.674372

[12] XIANG H., LI N., GAO J., ZHENG G., CHEN J., WANG C., ZHUANG S., *Comparison and applications of spherocylindrical, toroidal, and ellipsoidal surfaces for the correction of astigmatism in spectacle lenses*, Optics Express **28**(2), 2020: 1745-1757. https://doi.org/10.1364/OE.380700

[13] REMON L., TORNEL M., FURLAN W.D., *Visual acuity in simple myopic astigmatism: Influence of cylinder axis*, Optometry and Vision Science **83**(5), 2006: 311-315. https://doi.org/10.1097/01.opx.0000216099.29968.36

[14] KOBASHI H., KAMIYA K., SHIMIZU K., KAWAMORITA T., UOZATO H., *Effect of axis orientation on visual performance in astigmatic eyes*, Journal of Cataract & Refractive Surgery **38**(8), 2012: 1352-1359. https://doi.org/10.1016/j.jcrs.2012.03.032

[15] ATCHISON D.A., MATHUR A., *Visual acuity with astigmatic blur*, Optometry and Vision Science **88**(7), 2011: E798-E805. https://doi.org/10.1097/OPX.0b013e3182186bc4

[16] MATHUR A., SUHEIMAT M., ATCHISON D.A., *Pilot study: Effect of age on visual acuity with defocus and astigmatism*, Optometry and Vision Science **92**(3), 2015: 267-271. https://doi.org/10.1097/OPX.0000000000000459

[17] MIMOUNI M., NEMET A., POKROY R., SELA T., MUNZER G., KAISERMAN I., *The effect of astigmatism axis on visual acuity*, European Journal of Ophthalmology **27**(3), 2017: 308-311. https://doi.org/10.5301/ejo.5000890

[18] PUJOL J., ARJONA M., ARASA J., BADIA V., *Influence of amount and changes in axis of astigmatism on retinal image quality*, Journal of the Optical Society of America A **15**(9), 1998: 2514-2521. https://doi.org/10.1364/JOSAA.15.002514

[19] MILLER A.D., KRIS M.J., GRIFFITHS A.C., *Effect of small focal errors on vision*, Optometry and Vision Science **74**(7), 1997: 521-526.

[20] MALACARA Z., MALACARA-DOBLADO D., MALACARA-HERNANDEZ D., LANDGRAVE J., *Astigmatic optical surfaces, characteristics, testing, and differences between them*, Optical Engineering **46**(12), 2007: 123001. https://doi.org/10.1117/1.2818211

Received September 23, 2022
in revised form December 21, 2022